Biochemical and Biophysical Research Communications 441 (2013) 844–848

Contents lists available at ScienceDirect

Biochemical and Biophysical Research Communications

journal homepage: www.elsevier.com/locate/ybbrc

Bulkiness or aromatic nature of tyrosine-143 of actin is important for the weak binding between F-actin and myosin-ADP-phosphate

Yuki Gomibuchi [a], Taro Q.P. Uyeda [b], Takeyuki Wakabayashi [a,c,*]

[a] Graduate School of Science and Engineering, Teikyo University, Toyosatodai 1-1, Utsunomiya 320-8551, Japan
[b] Biomedical Research Institute, National Institute of Advanced Industrial Science and Technology, AIST Tsukuba Central 4, 1-1-1 Higashi, Tsukuba, Ibaraki 305-8562, Japan
[c] Department of Judo Therapy, Faculty of Medical Technology, Teikyo University, Toyosatodai 1-1, Utsunomiya 320-8551, Japan

ARTICLE INFO

Article history:
Received 16 October 2013
Available online 6 November 2013

Keywords:
Actin
Actin polymerizability
Actin-activated myosin ATPase
Weak interaction between actin and myosin
Dictyostelium actin
Aromatic nature
Bulkiness

ABSTRACT

Actin filaments (F-actin) interact with myosin and activate its ATPase to support force generation. By comparing crystal structures of G-actin and the quasi-atomic model of F-actin based on high-resolution cryo-electron microscopy, the tyrosine-143 was found to be exposed more than 60 Å^2 to the solvent in F-actin. Because tyrosine-143 flanks the hydrophobic cleft near the hydrophobic helix that binds to myosin, the mutant actins, of which the tyrosine-143 was replaced with tryptophan, phenylalanine, or isoleucine, were generated using the *Dictyostelium* expression system. It polymerized significantly poorly when induced by NaCl, but almost normally by KCl. In the presence of phalloidin and KCl, the extents of the polymerization of all the mutant actins were comparable to that of the wild-type actin so that the actin-activated myosin ATPase activity could be reliably compared. The affinity of skeletal heavy meromyosin to F-actin and the maximum ATPase activity (V_{max}) were estimated by a double reciprocal plot. The Tyr143Trp-actin showed the higher affinity (smaller K_{app}) than that of the wild-type actin, with the V_{max} being almost unchanged. The K_{app} and V_{max} of the Tyr143Phe-actin were similar to those of the wild-type actin. However, the activation by Tyr143Ile-actin was much smaller than the wild-type actin and the accurate determination of K_{app} was difficult. Comparison of the myosin ATPase activated by the various mutant actins at the same concentration of F-actin showed that the extent of activation correlates well with the solvent-accessible surface areas (ASA) of the replaced amino acid molecule. Because $1/K_{app}$ reflects the affinity of F-actin for the myosin–ADP-phosphate intermediate (M.ADP.Pi) through the weak binding, these data suggest that the bulkiness or the aromatic nature of the tyrosin-143 is important for the initial binding of the M.ADP.Pi intermediate with F-actin but not for later processes such as the phosphate release.

1. Introduction

The actin-filament system is required in many cytoplasmic processes including motility, cytokinesis, cell adhesion, cellular signaling, and intracellular trafficking. Although myosin is not required for the pseudopodia extension by actin polymerization, many other functions of actin filaments depend on their interaction with myosin.

Actin has two major domains separated by a nucleotide-binding cleft [1]. The outer domain is further divided into subdomains 1 and 2 and the inner domain into subdomains 3 and 4, with the subdomain 1 and 3 being separated by a hydrophobic cleft. By comparing the three-dimensional structure of F-actin and its complex with skeletal myosin subfragment-1 in the absence of ATP, it was determined that myosin binds mainly to the outer domain of the actin protomer on one strand of the actin double helix [2–6]. In the rigor complex, myosin binds to the hydrophobic helix of F-actin, which is located near the hydrophobic cleft between the subdomains 1 and 3. The importance of the hydrophobic cleft was highlighted by experiments using mutated myosin: it was found that three consecutive hydrophobic residues (Trp-546, Phe-547, and Pro-548) of myosin are important to interact with actin and that the target of these residues was proposed to be the segment including Tyr-143, Ala-144, Ser-145, and Gly-146 of actin [7], which flank the hydrophobic cleft of actin. It was also shown that the acidic residues including residues 1–4, Asp24, Asp25, Glu99, Glu100 of actin are essential for the ionic interaction with myosin [8,9]. From a biochemical point of view, there are two types of actin interactions with myosin: the weak binding with myosin.ADP.Pi and the strong binding with myosin–ADP or myosin without bound nucleotide. When muscle contraction is triggered by the increase in the intracellular calcium ion concentration,

* Corresponding author at: Department of Judo Therapy, Faculty of Medical Technology, Teikyo University, Toyosatodai 1-1, Utsunomiya 320-8551, Japan.
E-mail address: tw007@nasu.bio.teikyo-u.ac.jp (T. Wakabayashi).

0006-291X/$ - see front matter © 2013 Elsevier Inc. All rights reserved.
http://dx.doi.org/10.1016/j.bbrc.2013.10.144

myosin.ADP.Pi associates with actin–tropomyosin–troponin, and phosphate (Pi) is released so that the myosin ATPase cycle proceeds. We previously examined the effect of the de-acetylation at the amino-terminus of actin on actin-activated myosin ATPase. The affinity of deacetylated F-actin to myosin was significantly weaker (higher K_{app}) and it was suggested that the acetylation at N-terminus is important for the weak binding with myosin [10].

Recently F-actin structures based on high-resolution cryo-EM were reported [11–13]. When crystal structures of G-actin and our quasi-atomic model of F-actin are compared, the exposure of the majority of the residues in F-actin to solvent was less than that in G-actin due to the intermolecular interactions or unchanged. However, there were two exceptions. The calculated solvent-accessible surface area (ASA) of tyrosine-143 and tyrosine-240 increased in F-actin by more than 60 Å^2 [11]. In the case of the tyrosine-143, this exceptional increase in the ASA appeared to be linked with the widening of the hydrophobic cleft and the rotation of the outer domain against the inner one upon polymerization of actin [11]. We, therefore, mutated tyrosine-143 using *Dictyostelium* expression system [14], because (a) the activation of the myosin ATPase by F-actin is much higher than that by G-actin [15], (b) tyrosine-143 flanked the hydrophobic cleft near the hydrophobic helix (Fig. 1), which is proposed to be one of the myosin-binding sites.

The effects of the mutation of tyrosine-143 on the polymerizability and the capability to activate myosin ATPase were examined. The Tyr143Phe-actin showed poor polymerizability in the presence of NaCl as reported previously [11]. In the presence of phalloidin and KCl, all mutant actins polymerized almost normally so that the actin-activated ATPase could be compared. It was found that the bulkiness or the aromatic nature of the residue-143 is important for the activation of ATPase. The affinity of Tyr143Trp-actin to myosin.ADP.Pi intermediate was ~2 times higher than the wild-type actin, with V_{max} being almost unchanged.

2. Materials and methods

2.1. Expression and purification of proteins

Dictyostelium mutant actins and the wild-type actin were expressed and purified as described [14]. Briefly, mutant actins and the wild-type actin were expressed in *Dictyostelium* cells as a fusion protein with thymosin and a 6×His tag. The cells were suspended in 2 vol/g of binding buffer (10 mM imidazole–HCl (pH 7.4), 10 mM HEPES (pH 7.4), 300 mM NaCl, 2 mM $MgCl_2$, and 2 mM ATP) containing 2 mM benzamidine, 2 μg/mL leupeptin, 28.6 mM β-mercaptoethanol, 1 mM 4-(2-aminoethyl)benzenesulfonyl fluoridehydrocloride (AEBSF), 0.5 mM phenylmethylsulfonyl fluoride(PMSF), 0.01 mg/mL chymostatin, 0.01 mg/mL pepstatin, and 2 mg/mL TLCK after they were collected and washed twice with 17 mM Na–K phosphate buffer (pH 6.5) at 4 °C. The suspended cells were sonicated 6 times for 10 s, centrifuged at 10,500×*g* for 15 min, and then ultracentrifuged 142,000×*g* for 1 h. The resultant supernant was applied to Ni Sepharose high performance gel (GE Healthcare) pre-equilibrated with washing buffer (10 mM imidazole–HCl (pH 7.4), 10 mM HEPES (pH 7.4), 300 mM NaCl, 0.5 mM $MgCl_2$, and 0.1 mM ATP), and bound proteins were eluted with linear 10–500 mM imidazole gradient. The resultant fusion protein fraction was dialyzed against G-buffer (2 mM Tris–HCl (pH 7.4), 0.2 mM $CaCl_2$, 0.2 mM ATP, and 0.5 mM DTT) and then digested with α-chymotrypsin (200:1 w/w) for 5–10 min at 25 °C. After quenching the reaction with 4 mM AEBSF and 0.02 mg/mL chymostatin/pepstatin mixture, the digested mixture was applied to a DEAE-5PW column pre-equilibrated with G-buffer, and bound proteins were eluted with linear 0–0.5 M NaCl gradient in G-buffer. The eluted G-actin fraction was applied to a Superdex 75 column equilibrated with G-buffer. The peak fractions were pooled and concentrated using Amicon ultra-4. Myosin was prepared from rabbit skeletal muscle. Heavy meromyosin (HMM) was obtained by digesting myosin with chymotrypsin following the procedure described previously [16]. Protein concentration of HMM was measured by absorbance at 280 nm and that of actin was measured using proteostain (Dojindo Molecular Technologies. Inc.). The value obtained by the proteostain method was calibrated by absorbance at 280 nm [17].

2.2. Polymerization assay

G-actin (2.3 μM) was incubated in 150 mM KCl or NaCl, 20 mM imidazole–HCl (pH 7.0), 3 mM $MgCl_2$, 10 μM $CaCl_2$, and 1 mM ATP for 30 min at 25 °C, and ultracentrifuged. The pellet was suspended with 150 mM NaCl and 20 mM imidazole–HCl (pH 7.0) and then analyzed by SDS–PAGE [11]. Gels were stained with Coomassie Brilliant Blue, scanned, and quantified using ImageJ [18].

2.3. Actin-activated HMM ATPase measurement

Actin-activated HMM ATPase was measured as described [10]. In brief, the reaction solution contained 2.5 mM KCl, 10 mM imidazole–HCl (pH 7.0), 4 mM $MgCl_2$, 1 mM ATP, 5 μg/mL phalloidin, 0.03 mg/mL skeletal HMM, and G-actin (0–25 μM) at 25 °C. Liberated phosphate was measured by the malachite green method [19].

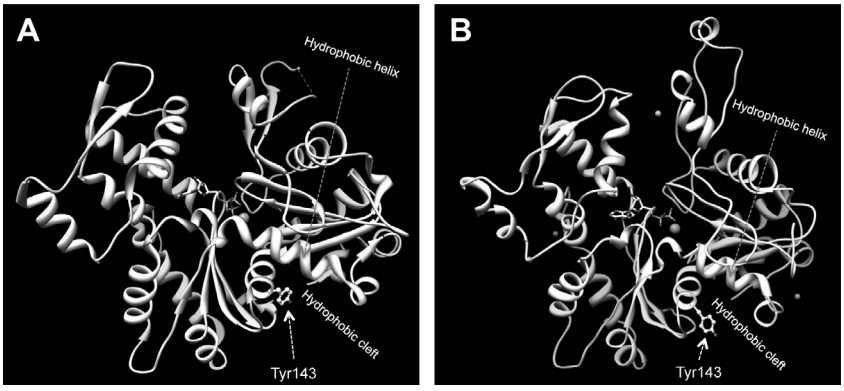

Fig. 1. Overviews of the actin structures. The tyrosine-143 is shown as a ball-and-stick model. (A) G-actin structure of the wild-type *Dictyostelium* actin (PDB: 1C0F) [21] (B) Rabbit skeletal F-actin (PDB: 3G37) [11]. Figures were prepared using UCSF Chimera [22].

3. Results

3.1. Polymerizability of Tyr143-mutant actins

Fig. 2 shows the polymerizability of actins triggered by NaCl (left panels) or KCl (right panels) without (upper panels) or with (lower panels) phalloidin. The polymerizability of Tyr143Phe-actin deceased to ~45% of the wild-type actin, when the extent of polymerization was measured at 30 min after triggering polymerization by adding NaCl as shown in Fig. 2A. Tyr143Trp-actin (~66%) and Tyr143Ile-actin (~58%) also showed a similar tendency. The tyrosine-143 appeared more exposed to the solvent after polymerization and flanks the hydrophobic cleft that widened after polymerization, and these processes may have been impaired by the introduction of a more hydrophobic side chain. However, the extent of polymerization was sensitive to species of cations. The polymerization of Tyr143Phe-actin induced by KCl was almost the same as the wild-type actin, whereas Tyr143Ile-actin still showed poorer polymerizability (~50%) as shown in Fig. 2B.

In the presence of phalloidin, all the mutant actins showed almost normal polymerization in the presence of NaCl (Fig. 2C) or KCl (Fig. 2D). Under the conditions for the ATPase assay in the presence of phalloidin and KCl, the polymerizability of the Tyr143-Phe-actin, Tyr143Trp-actin, and Tyr143Ile-actin were ~92.5%, ~112.9%, and ~116.3% of that of the wild-type actin, so that the small difference in the extent of polymerization can be compensated for before comparing double reciprocal plots. We compared two ways for compensating the small difference in the polymerizability: one way is to compensate the ATPase activity, and the other to compensate the actin concentration. Although both gave similar results, we compensated the actin concentration to analyze double reciprocal plots (Fig. 3). However, the ATPase activity was compensated before the analysis of correlation between the ATPase activity and the solvent-accessible surface area (ASA) (Fig. 4).

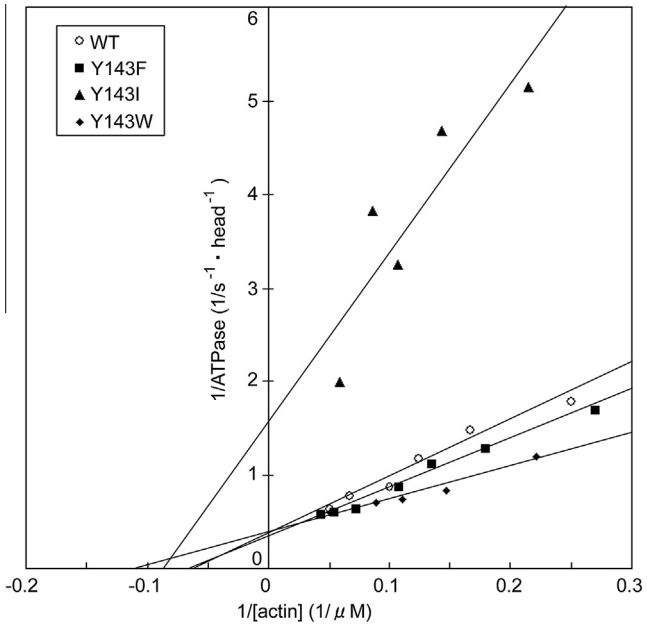

Fig. 3. A double reciprocal plot (Lineweaver–Burk type) of the actin-activated ATPase activity with the wild-type actin (open circle), the Tyr143Phe-actin (filled square), Tyr143Trp-actin (filled diamond), and Tyr143Ile-actin (filled triangle). The ATPase activity was measured in 2.5 mM KCl, 10 mM imidazole–HCl (pH 7.0), 4 mM $MgCl_2$, 1 mM ATP, 5 μg/mL phalloidin, 0.03 mg/mL HMM, and various concentrations of actin (from 4 to 25 μM) at 25 °C. The intercepts on the ordinate and the abscissa represent $1/V_{max}$ and $-1/K_{app}$, respectively. The K_{app} for Tyr143Trp-actin was the smallest (7.21 μM), whereas those for the wild-type actin and Tyr143Phe-actin were 15.3 and 16.4 μM, respectively. For Tyr143Ile-actin, the K_{app} could not be determined reliably due to the weak activation. The V_{max}'s for the wild-type actin, Tyr143Phe-actin, and Tyr143Trp-actin were 2.67, 2.78, 2.83 $s^{-1}head^{-1}$, respectively and did not differ much, whereas that for Tyr143Ile was smaller than 1 $s^{-1}head^{-1}$.

3.2. Activation of myosin ATPase activity by mutant actins

The actin-activated ATPase activity was measured using skeletal heavy meromyosin (HMM) under low ionic strength conditions. The actin-activated activity was calculated by subtracting the basal ATPase of HMM under the same reaction conditions. The small differences in the polymerizability among mutant actins were compensated for by compensating the actin concentration according to the extents of polymerization so that the values can be compared with that for the wild-type actin.

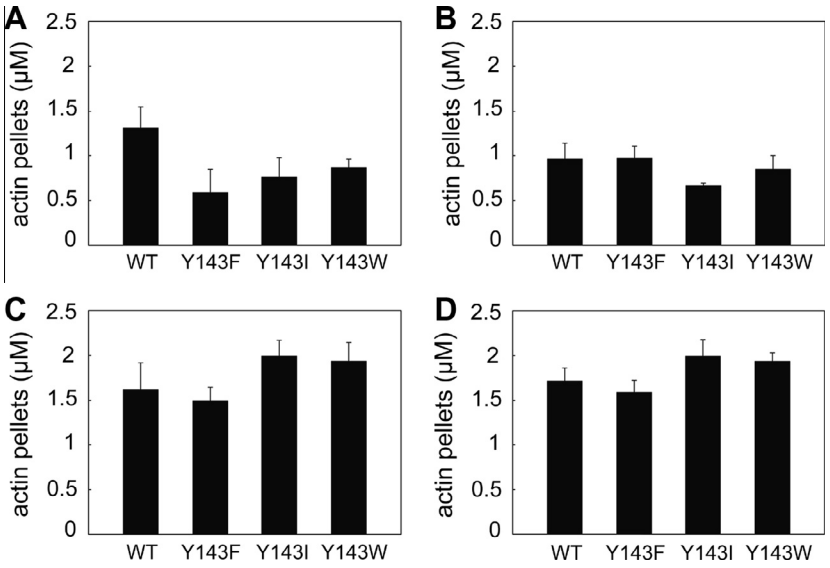

Fig. 2. Polymerizability of actins triggered by NaCl (left panels) or KCl (right panels) without (upper panels) or with (lower panels) phalloidin. Actins (2.3 μM) were incubated for 30 min at 25 °C, ultracentrifuged, and analyzed by SDS–PAGE. The data represent mean values with standard errors of the amount of actin in pellets. (A) Polymerization was triggered by NaCl. (B) Polymerization was triggered by KCl. (C) Polymerization was triggered by NaCl in the presence of 5 μg/mL phalloidin. (D) Polymerization was triggered by KCl in the presence of 5 μg/mL phalloidin.

Fig. 3 shows the double reciprocal plots of 1/ATPase versus 1/[F-actin] (Lineweaver–Burk type). The double reciprocal plots for the wild-type actin, Tyr143Trp-actin, and Tyr143Phe-actin appeared to be linear. However, the linearity was not clear for Tyr143Ile-actin due to much lower activation (~1/3 of the wild-type actin). The V_{max}'s of the actin-activated ATPase activities by the wild-type actin, Tyr143Trp-actin, and Tyr143Phe-actin were similar: 2.67, 2.32, and 3.00 $s^{-1}head^{-1}$, respectively. Although the V_{max} for Tyr143Ile-actin could not be obtained accurately, it was estimated to be less than ~1 $s^{-1}head^{-1}$.

The phosphate release from the myosin.ADP.Pi intermediate is a rate-limiting step of the myosin ATPase cycle. F-actin accelerates this step by binding weakly to the myosin.ADP.Pi intermediate. Therefore, the affinity of F-actin to the myosin.ADP.Pi intermediate can be estimated by the analysis of a double reciprocal plot: the affinity is the reciprocal of K_{app}, which is the concentration of F-actin at which half maximal activation occurs. The affinity of Tyr143Trp-actin was about two times higher than that for the wild-type actin. In term of K_{app}, the values for Tyr143Trp-actin and the wild-type actin were 7.2 and 15.3 μM, respectively. The K_{app} for Tyr143Phe-actin was 16.4 μM and comparable with that for the wild-type actin. For Tyr143Ile-actin, the reliable value could not be obtained due to the lower activation. These data suggest that the tryptophan at the position of the residue-143 enhances the weak binding with the myosin.ADP.Pi intermediate.

Fig. 4 shows the correlation of the bulkiness of the side chain introduced to the residue-143 of mutant actins with the actin-activated myosin ATPase at various concentrations of F-actin. As an index of bulkiness, the solvent-accessible surface area (ASA) of the amino acid molecule was chosen, because it correlates well with the bulkiness of the amino acid residues [20]. At each of the concentrations of F-actin, the ATPase activation correlates well with the molecular ASA. These data suggest that the bulkiness of the residue-143 is important for the activation of myosin ATPase. Amino acids with a bulky side chain are either branched at the β-carbon atom (Val, Ile, and Thr) or with a large aromatic ring (Phe, Tyr, Trp). Therefore, we cannot exclude the possibility that the aromatic nature of the residue-143 may be important.

4. Discussion

This study showed the importance of tyrosine-143 of actin for the polymerizability and for the activation of myosin ATPase. As shown in Fig. 1, this residue is located next to the loop, which is located near the boundary between the outer and inner domains. It flanks the hydrophobic cleft, which appears to be widened upon polymerization [11]. Importantly, this tyrosine is conserved among various actin isoforms across the eukaryotic species including *Dictyostelium*, rabbit, and human.

The widening of the hydrophobic cleft and the increase in the ASA of the side chain of the tyrosine-143 upon polymerization prompted the idea that these structural changes may be hindered by replacing the residue-143 with a more hydrophobic residue. In this case the polymerization process also may be hindered. As expected, the mutant actins showed poorer polymerizability in the presence of NaCl. Particularly, the Tyr143Phe-actin differs from the wild-type actin only by one oxygen atom, but the polymerization became about one half.

The actin-activated myosin ATPase was measured using the skeletal heavy meromyosin (HMM) from rabbit. Fortunately, all the actin mutants polymerized normally in the presence of

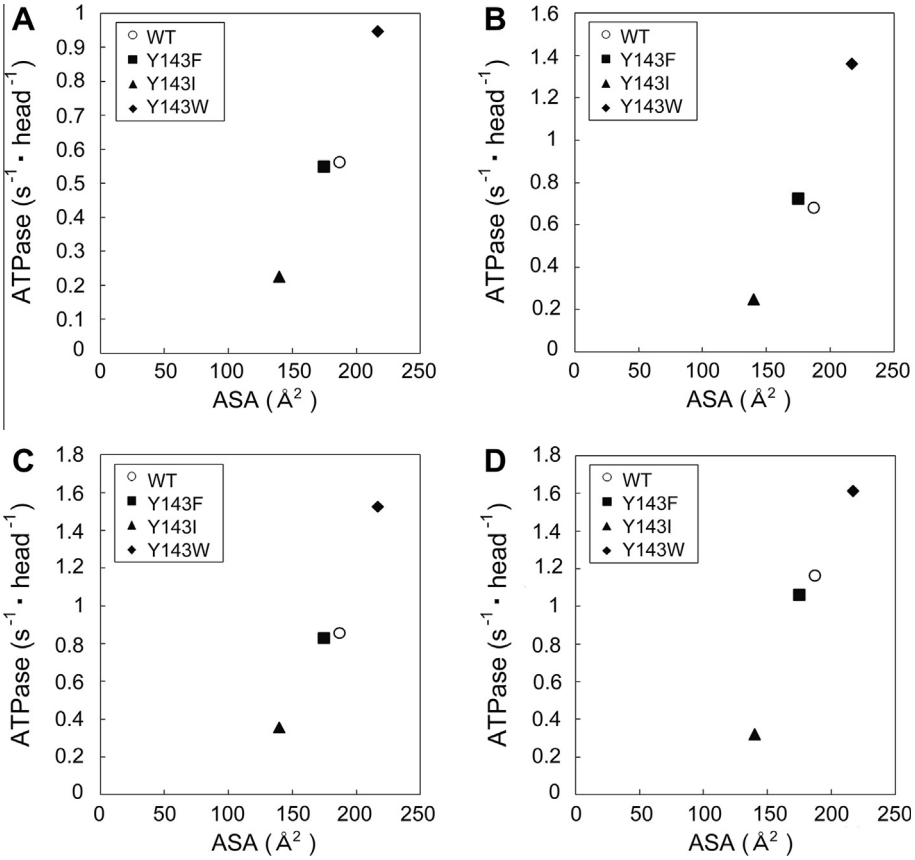

Fig. 4. The correlation of the actin-activated myosin ATPase with the solvent-accessible surface area (ASA) of the amino acid molecules at the residue-143. The actin-activated myosin ATPase activity correlates well with molecular ASA, which also correlates well with the bulkiness of the residue [19]. Actin concentration was (A) 4 μM, (B) 6 μM, (C) 8 μM, or (D) 10 μM.

phalloidin, which suppresses the depolymerization of F-actin, so that their activation of myosin ATPase could be compared with the wild-type actin. The Tyr143Ile-actin activated HMM ATPase poorly. It indicates that the bulkiness of the residue-143 is important as shown in Fig. 4: the extent of the ATPase activation correlates well with the solvent-accessible surface area, which in turn correlates with bulkiness, of the replaced amino acid residue. Amino acids with a bulky side chain include those branched at the β-carbon atom (Val, Ile, and Thr) or those with a large aromatic ring (Phe, Tyr, and Trp). Because there is no aliphatic amino acid that is larger than aromatic amino acids, it is difficult to exclude the importance of the aromatic nature. Moreover, the hydrophobic cleft of actin is flanked also with many other aromatic residues.

We showed that the tyrosine-143 is involved in the weak binding with myosin and that the bulkiness or the aromatic nature of tyrosine-143 is important for ATPase activation. Previously, the electrostatic interactions between F-actin and myosin have been shown to be important for the weak binding: the actin-activated myosin ATPase becomes weaker at higher ionic strength and the charge-reversion of Glu360/Glu361 or Asp363/Glu364 of actin resulted in an increase of K_{app}. Our results show that the importance of the non-electrostatic interaction for the weak binding between F-actin and myosin.ADP.Pi.

The Tyr143Trp-actin showed lower K_{app} of the actin-activated myosin ATPase reflecting the higher affinity to the myosin.ADP.Pi intermediate. So far it has been difficult to study the weak binding between myosin.ADP.Pi and F-actin due to the weakness of the interaction. This mutant actin would prove useful to clarify the nature of the weak binding, which is an initial step for activating the ATPase cycle of myosin, which is essential for force generation.

Acknowledgments

We thank Kenji Murakami for help on the development of the biochemical systems. This work was supported by a grant-in-aid for Scientific Research and a grant-in-aid for Scientific Research on Priority Areas (Water and ATP) from the Ministry of Education, Culture, Sports, Science and Technology of Japan.

References

[1] W. Kabsch, H.G. Mannherz, D. Suck, E.F. Pai, K.C. Holmes, Atomic structure of the actin:DNase I complex, Nature 347 (1990) 37–44.
[2] C. Toyoshima, T. Wakabayashi, Three-dimensional image analysis of the complex of thin filaments and myosin molecules from skeletal muscle. V. Assignment of actin in the actin–tropomyosin–myosin subfragment-1 complex, J. Biochem. 97 (1985) 245–263.
[3] R.A. Milligan, P.F. Flicker, Structural relationships of actin, myosin, and tropomyosin revealed by cryo-electron microscopy, J. Cell Biol. 105 (1987) 29–39.
[4] I. Rayment, H.M. Holden, M. Whittaker, C.B. Yohn, M. Lorenz, K.C. Holmes, R.A. Milligan, Structure of the actin–myosin complex and its implications for muscle contraction, Science 261 (1993) 58–65.
[5] R.R. Schroder, D.J. Manstein, W. Hahn, H. Holden, I. Rayment, K.C. Holmes, J.A. Spudich, Nature 364 (1993) 171–174.
[6] E. Behrmann, M. Mueller, P.A. Penczek, H.G. Mannherz, D.J. Manstein, S. Raunser, Structure of the rigor actin–tropomyosin–myosin complex, Cell 150 (2012) 327–338.
[7] H. Onishi, S.V. Mikhailenko, M.F. Morales, Toward understanding actin activation of myosin ATPase: the role of myosin surface loops, Proc. Natl. Acad. Sci. USA 103 (2006) 6136–6141.
[8] K. Sutoh, M. Ando, K. Sutoh, Y.Y. Toyoshima, Site-directed mutations of *Dictyostelium* actin: disruption of a negative charge cluster at the N terminus, Proc. Natl. Acad. Sci. USA 88 (1991) 7711–7714.
[9] M. Johara, Y.Y. Toyoshima, A. Ishijima, H. Kojima, T. Yanagida, K. Sutoh, Charge-reversion mutagenesis of *Dictyostelium* actin to map the surface recognized by myosin during ATP-driven sliding motion, Proc. Natl. Acad. Sci. USA 90 (1993) 2127–2131.
[10] A. Abe, K. Saeki, T. Yasunaga, T. Wakabayashi, Acetylation at the N-terminus of actin strengthens weak interaction between actin and myosin, Biochem. Biophys. Res. Commun. 268 (2000) 14–19.
[11] K. Murakami, T. Yasunaga, T.Q.P. Noguchi, Y. Gomibuchi, K.X. Ngo, T.Q.P. Uyeda, T. Wakabayashi, Structural basis for actin assembly, activation of ATP hydrolysis, and delayed phosphate release, Cell 143 (2010) 275–287.
[12] T. Fujii, A.H. Iwane, T. Yanagida, K. Namba, Direct visualization of secondary structures of F-actin by electron cryomicroscopy, Nature 467 (2010) 724–728.
[13] V.E. Galkin, A. Orlova, G.F. Schroeder, E.H. Egelman, Structural polymorphism in F-actin, Nat. Struct. Mol. Biol. 17 (2010) 1318–1323.
[14] T.Q.P. Noguchi, N. Kanzaki, H. Ueno, K. Hirose, T.Q.P. Uyeda, A novel system for expressing toxic actin mutants in *Dictyostelium* and purification and characterization of a dominant lethal yeast actin mutant, J. Biol. Chem. 282 (2007) 27721–27727.
[15] G. Offer, H. Baker, L. Baker, Interaction of monomeric and polymeric actin with myosin subfragment 1, J. Mol. Biol. 66 (1972) 425–444.
[16] Y. Okamoto, T. Sekine, A streamlined method of subfragment one preparation from myosin, J. Biochem. 98 (1985) 1143–1145.
[17] T.W. Houk, K. Ue, The measurement of actin concentration in solution: a comparison of methods, Anal. Biochem. 62 (1974) 66–74.
[18] C.A. Schneider, W.S. Rasband, K.W. Eliceiri, NIH image to imagej: 25 years of image analysis, Nature Methods 9 (2012) 671–675.
[19] T. Kodama, K. Fukui, K. Kometani, The initial phosphate burst in ATP hydrolysis by myosin and subfragment-1 as studied by modified malachite green method for determination of inorganic phosphate, J. Biochem. 99 (1986) 1465–1472.
[20] S. Miller, J. Janin, A.M. Lesk, C. Chothia, Interior and surface of monomeric proteins, J. Mol. Biol. 196 (1987) 641–656.
[21] Y. Matsuura, M. Stewart, M. Kawamoto, N. Kamiya, K. Saeki, T. Yasunaga, T. Wakabayashi, Structural basis for the higher Ca^{2+}-activation of the regulated actin-activated myosin ATPase observed with *Dictyostelium*/tetrahymena actin chimeras, J. Mol. Biol. 296 (2000) 579–595.
[22] E.F. Pettersen, T.D. Goddard, C.C. Huang, G.S. Cough, D.M. Greenblatt, E.C. Meng, T.E. Ferrin, UCSF chimera – a visualization system for exploratory research and analysis, J. Comput. Chem. 25 (2004) 1605–1612.